Modeling radiative-shocks created by laser- cluster interactions

R H H Scott, N Booth, S J Hawkes, D R Symes, C Hooker, H. W Doyle, S I Olsson-Robbie, H F Lowe, C J Price, D. Bigourd, et al.

Modeling radiative-shocks created by laser–cluster interactions

Cite as: Phys. Plasmas **27**, 033301 (2020); https://doi.org/10.1063/1.5136070
Submitted: 12 November 2019 . Accepted: 05 February 2020 . Published Online: 02 March 2020

R. H. H. Scott, N. Booth, S. J. Hawkes, D. R. Symes, C. Hooker, H. W. Doyle, S. I. Olsson-Robbie, H. F. Lowe, C. J. Price, D. Bigourd, S. Patankar, K. Mecseki, E. T. Gumbrell, and R. A. Smith

Physics of Plasmas ARTICLE scitation.org/journal/php

Modeling radiative-shocks created by laser–cluster interactions

Cite as: Phys. Plasmas **27**, 033301 (2020); doi: 10.1063/1.5136070
Submitted: 12 November 2019 · Accepted: 5 February 2020 ·
Published Online: 2 March 2020

R. H. H. Scott,[1,a)] N. Booth,[1] S. J. Hawkes,[1] D. R. Symes,[1] C. Hooker,[1] H. W. Doyle,[2] S. I. Olsson-Robbie,[3] H. F. Lowe,[3] C. J. Price,[3] D. Bigourd,[4] S. Patankar,[5] K. Mecseki,[6] E. T. Gumbrell,[7] and R. A. Smith[3]

AFFILIATIONS

[1]Central Laser Facility, STFC Rutherford Appleton Laboratory, Harwell Oxford, Didcot OX11 0QX, United Kingdom
[2]First Light Fusion, Mead Rd., Yarnton, Kidlington OX5 1QU, United Kingdom
[3]Department of Physics, The Blackett Laboratory, Imperial College London, London SW7 2AZ, United Kingdom
[4]IMS Bordeaux University, UMR CNRS 5218, Bat. A31, 351 Cours de la Liberation, 33400 Talence, France
[5]Lawrence Livermore National Laboratory, P.O. Box 808, Livermore, California 94550, USA
[6]SLAC National Accelerator Laboratory, 2575 Sand Hill Rd., Menlo Park, California 94025, USA
[7]Plasma Physics Division, AWE Aldermaston, Reading RG7 4PR, United Kingdom

[a)]**Electronic mail:** robbie.scott@stfc.ac.uk

ABSTRACT

Radiative-shocks induced by laser–cluster interactions are modeled using radiation-hydrodynamic simulations. A good agreement—in both shock velocity and density profiles—is obtained between experiment and simulations, indicating that non-local thermodynamic equilibrium (NLTE) radiative effects are important in the experimental regime examined, particularly at early times ($\lesssim$30 ns) due to the elevated temperatures ($\gtrsim$35 eV). The enhanced NLTE radiative emission causes the shock to be reduced in amplitude, increased in width, and reduced in propagation velocity, while the amplitude of the radiative precursor is increased. As the density and temperature conditions are relatively modest, this potentially has important implications for the scalings that are used in laboratory–astrophysics to transform between laboratory and astrophysical scales, which do not hold for non-LTE systems.

I. INTRODUCTION

The mathematical models governing radiation-hydrodynamics are scale-invariant under the appropriate transformations and assumptions.[1] Consequently, experiments of relevance to astrophysical systems can be performed within the laboratory, despite the huge differences in spatiotemporal scales between the two systems. Today's laser systems enable the generation of plasmas, which are in regimes of relevance to certain scaled astrophysical systems. Here, we numerically investigate the dynamics of radiative-shocks in laboratory scale laser–cluster experiments, comparing experiments and simulation, with a particular emphasis on the atomic models used to generate the opacity data [LTE/steady state non-LTE (NLTE)/collisional–radiative (CR) non-LTE] and their effects on the radiative-shock's characteristics.

Shock waves are particularly interesting astrophysical systems, as they are ubiquitous throughout the universe and play a crucial role in the transport of energy into the interstellar medium[2] and the generation of high-energy cosmic rays.[3,4] In the limit of a weak shock, the role of radiation in the shock's energy balance is small, and the pressure, density, and temperature profiles across the shock have the classical step-like characteristics of a purely hydrodynamic shock. However, as the shock strength and hence downstream temperature increase, the radiation flux from the shock's front surface will increase rapidly [assuming local thermodynamic equilibrium (LTE), the radiative flux is proportional to σT^4, where σ is the Stephan–Boltzmann constant and T is the electron temperature]. The emitted radiation is absorbed by the upstream material over a distance of the order of the photon mean-free-path. The absorption of the photons heats the upstream material, potentially creating a "shelf" or precursor in temperature and pressure, which precedes the shock front, changing the upstream conditions sufficiently to begin to modify the shock propagation dynamics. Importantly, the photon absorption may also cause electron

excitation and ionization of the upstream media, and this, in turn, modifies the local emissivity and opacity, creating a complex system where radiation transport plays a crucial role in the energy balance of the system as a whole. As the free electron density level may be elevated upstream of the shock (a radiative precursor), this provides an experimental observable that the shock is radiating at an energetically significant level. Such systems are called radiative-shocks,[5–8] and they have been observed around a wide variety of astronomical objects, e.g., accretion shocks, pulsating stars, supernovae in their radiative cooling stage, bow shocks of stellar jets in the galactic medium, collisions of interstellar clouds, entry of rockets or comets into planetary atmospheres, and, on a laboratory scale, in laser–gas interactions[9,10] and in the late time disassembly of inertial confinement fusion capsules.[11] For a given pressure, radiative-shocks occur more readily in lower density media, as the temperature ($\propto 1/\rho$), and hence radiative flux ($\propto T^4/\rho$ in LTE), will be higher.

Atomic clusters are created in the laboratory by the rapid adiabatic expansion of gas into a vacuum.[12] The resulting drop in temperature condenses the gas into clusters of size $\sim 10-100$ nm. On a microscopic scale, the ionized clusters are over-dense to optical laser light, while the "cluster gas" is macroscopically under-dense. The laser energy is absorbed locally to the over-dense clusters. Due to the spherical structure of the clusters, the laser's electric field excites a resonantly driven oscillation of the (partially ionized) cluster's electrons.[13] This resonance occurs when the light frequency is near to the cluster's plasma frequency and causes an associated resonance in the optical absorption spectrum.

Laser–cluster experiments, e.g., Refs. 9 and 14–16 and references therein, report high laser absorption fractions into thin filaments of width of the order of the laser focal spot size. The generation of a thin, hot filament of plasma, in turn, creates a cylindrical blast wave,[17] where a sudden release of energy from a region of small-spatial-extent causes an expanding shock to sweep up material ahead of the shock. By increasing the material's atomic number Z, and hence Z^* (the ionization state), the radiative properties of the shock can be controlled for a given shock temperature.

When a plasma is at *thermodynamic equilibrium*, the whole system, composed of electrons, atoms, ions, and radiation, can be fully described by statistical mechanics, with each of the particle distributions described by the same characteristic temperature T. Here, the *electron energy distribution function* (EEDF) is a Maxwellian of temperature T, while the relative population of the excited states, the *atomic state distribution function* (ASDF), is populated in Saha–Boltzmann equilibrium at the temperature and density concerned, and the radiation field is described by the Planck function at T. Under thermodynamic equilibrium, each electron state transition process is balanced by its inverse process and the systems are said to be in *detailed balance*. However, this is often not the case since the plasma must be sufficiently large such that the optical depth for all emitted radiation frequencies is significantly less than the plasma spatial scale at all points in the plasma in order for the equilibrium state to be established.

Gradients in space and/or time can cause photons to escape from the plasma, and this, in turn, causes the radiative energy distribution function to deviate from the Planck function, affecting the detailed balance of electrons, ions, and atomic states. In principle, the system is no longer in thermodynamic equilibrium; if, however, the energy lost due to radiation is relatively small compared to the overall energy balance, the Saha–Boltzmann and Maxwellian distributions are still approximately valid locally and the system is said to be in *local thermodynamic equilibrium* (LTE), in which case $T_{ASDF} = T_e = T_i \neq T_r$, where T_{ASDF} is the temperature characterizing the excited states and T_e, T_i, and T_r are the electron, ion, and radiation temperatures, respectively. A further departure from thermodynamic equilibrium occurs when $T_e \neq T_i$, in such systems $T_{ASDF} \sim T_e$.[18]

As a general rule, a plasma is said to *not* be in equilibrium if the rate of photon absorptions $\gg$ rate of electron collisions. The commonly used McWhirter criterion[19] indicates that the ratio of the rate of electron collisions to the rate of photon absorptions should be at least 10. This can be expressed by the relation[18] $n_e(\mathrm{cm}^3) > 1.6 \times 10^{12} T_K^{1/2} \Delta E_{\mathrm{eV}}^3$, where n_e is the electron number density T_K in K and ΔE_{eV} is the largest energy gap between adjacent levels in eV. However, as discussed in a comprehensive recent work by Cristoforetti *et al.*,[18] this criterion can only rigorously be applied in a stationary, homogeneous plasma that is optically thin. For these circumstances, if this criterion is *not* fulfilled, LTE *cannot* be true; importantly, however, even then it only indicates when LTE *may* be true, rather than when LTE *is* true. Nonetheless, a system is more likely to be in LTE if the density is high and the temperature is low.

In the case of time-dependent and inhomogeneous plasmas, two further criteria should be verified.[18] First to account for the transient nature of the plasma, the temporal variation of thermodynamic parameters should be small over the excitation and ionization equilibration timescales. Second, the scale length of variations in electron temperature and number density in the plasma should be larger than the scale length of the particle diffusion over the time it takes for the plasma to relax to equilibrium. When spatial and/or temporal gradients are strong or when radiative processes significantly affect the overall energy balance, the system still further departs from thermodynamic equilibrium, usually requiring a space and time resolved collisional–radiative (CR) model[20] to obtain a solution. Here, various radiative and collisional processes (and their inverses) that take place between electrons, ions, and photons must be considered. In order to calculate the populations of the numerous energy levels, a large number of coupled rate equations are solved, requiring an iterative approach. This must be solved simultaneously with the radiative transfer equation. For higher Z elements, this can be an extremely challenging calculation given the huge numbers of energy levels, transitions, cross sections, etc., involved.

Self-consistent modeling of the generation and subsequent propagation of radiative-shocks generated by laser–cluster interactions is extremely challenging due to the disparate spatial and temporal scales of the various aspects of the interaction: the cluster sizes are $\leq$100 nm, while the shock propagates over $\sim$1 cm; the driving laser duration is 40 fs, while that of the shock propagation measurements is $\sim$100 ns. The complex kinetics, which dominates the high-intensity laser–cluster interactions could, in principle, be captured by particle-in-cell (PIC) simulations; however, the computation overheads of PIC techniques, combined with numerical issues associated with running for long timescales, mean that it would not be feasible to run to the tens of nanoseconds of the experimentally measured radiative-shock propagation. Furthermore, due to the relatively simple ionization models and the lack of radiation transport models in most PIC codes, this technique is unlikely to capture anything other than the most simple atomic kinetics and certainly not the effects of detailed opacity and

re-emitted radiation. Consequently, no attempt has been made in this work to directly simulate the laser–cluster interaction that governs the initial short-time scale energy deposition into the system.

As the principal aim of the modeling described in Secs. II and III was to attempt to reproduce and better understand the experimental observations, a pragmatic approach was adopted, which initializes radiation-hydrodynamics simulations using initial conditions based upon the experimental observations. One dimensional radiation-hydrodynamics simulations have been performed in cylindrical geometry using the radiation-hydrodynamics code Hyades,[23] as described in Sec. II.

II. NON-LTE MODELING OF RADIATIVE-SHOCK EXPERIMENTS

This section describes the application of LTE and non-LTE radiation-hydrodynamic modeling to a dataset obtained during an experimental campaign, detailed by Osterhoff *et al.* in Ref. 16. Briefly, the experimental characteristics were as follows: an $f/7$ spherical mirror focused into a plume of xenon clusters with an intensity of up to 1×10^{18} W/cm^2, creating a hot plasma filament approximately 65 μm in diameter and 4 mm long, which developed into a strong cylindrical blast wave. Xenon clusters were irradiated with 440 mJ per pulse and an average gas density of 1.6×10^{-4} g cm^{-3}. Time resolved interferometry was the principal diagnostic, giving an absolute measure of the free electron density at various discrete times.

The solid lines in Fig. 1 depict the interferometrically inferred experimental free electron density at various times. Upstream of the shock front (to the right), the free electron density is raised significantly above the background density (initial ion number density is 7.3×10^{17} cm^{-3}), this is caused by ionization of the upstream material by photons emitted from the shock front. Reproducing this experimental data with simulations proved very challenging, as it is highly constrained by both the experimental initial conditions and subsequent observations—the bulk energetics are constrained by the shock radius and velocity, while the details of the ionization and associated radiation transport dictate the radiation emission and the structure of the radiative precursor, which, in turn, feedback into the shock profile and strength. The presence of the radiative precursor provides a clear indication that the upstream plasma is not completely optically thin to the radiation emitted by the shock and/or downstream material, as it is the coupling of this radiation which heats the material upstream of the main shock front, locally raising the ionization level and hence the free electron density; this is visible experimentally as the precursor.

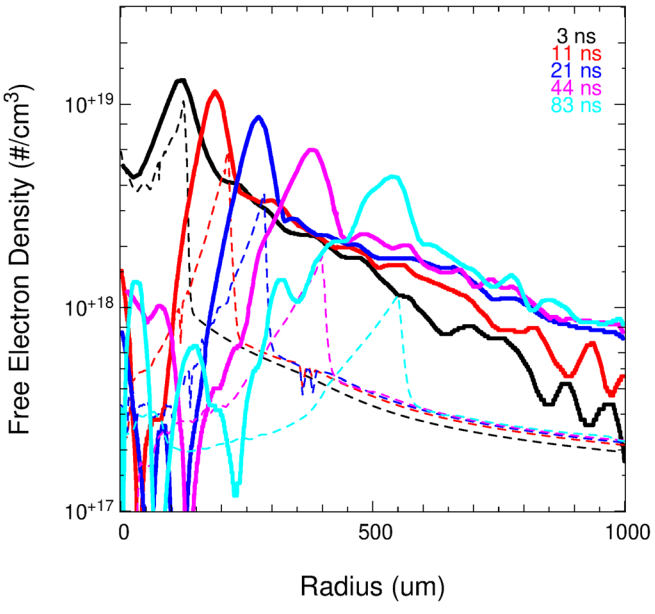

FIG. 1. Hyades steady state non-LTE simulation data (dotted lines) over plotted on the experimental data (solid lines). In this simulation, which uses the nominal experimental density, the amplitude of the radiative precursor (shown on the right of the figure) is under-predicted.

In order to reproduce the experimental data, a search of the parameter space was performed using Hyades[23] in cylindrical geometry with differing opacity/atomic models. The SESAME equation of state was used throughout. The parameter space searches included variations in initial density, filament radius, and internal energy. Variations from the experimental values were confined to approximately a factor of 5 around the nominal experimentally measured values. The Hyades runs were initialized by distributing the internal energy with a radial Gaussian spatial profile within the electron population via the electron temperature, in order to accurately reflect the initial laser energy deposition into the electrons. An inherently kinetic characteristic of laser–cluster interactions is the rapid transfer of electron energy to the ions. This was not represented within these hydrodynamic simulations and is justified on the basis that the electron-ion equilibration time scale is significantly less than that of the shock-evolution time scale. Radiation transport was modeled using the multi-group diffusive approximation. A range of atomic kinetics/opacity models were employed: LTE, steady-state non-LTE, and time-dependent non-LTE (full collisional–radiative).

A close, but not exact, match of both the measured free electron density profiles and the shock trajectory was obtained. In order to best match the data, the initial density was set to that of the experiment, the filament radius was 50 μm full-width-at-half-maximum (approximately, the experimental laser focal spot size), while the internal energy initially deposited in the electrons was tuned by changing the ion and/or electron temperature. LTE, steady-state non-LTE, and time-dependent non-LTE (CR) atomic models were used in order to find a best match to the data. When using the experimental background density and a peak electron temperature of 400 eV (internal energy 0.11 J), the principal discrepancy between simulation and experiment is in the width of the peak and the amplitude of the radiative precursor, as shown in Fig. 1. Assuming that all of the absorbed laser energy went into internal energy and was not lost to, e.g., Coulomb explosion of the clusters, this implies a relatively small absorption fraction of ~25% in comparison to experimental data (>50%). This energy deficit may be explained by a fraction of the absorbed laser energy being transferred to non-thermal ions during the laser–cluster interaction, and such populations are regularly observed in laser–cluster interactions.

In order to increase the coupling of the radiation emitted by the shock to the upstream material, the initial background gas density was artificially increased to 5×10^{-4} g cm^{-3} (3.1× the value measured off-line). Due to the increase in density, the filament internal energy was 0.3 J in this simulation; at 68%, this compares favorably with the

>50% laser absorption routinely reported in cluster experiments. The steady-state non-LTE modeling obtained using these parameters is shown in Figs. 2(b) and 2(e).

An R^2 analysis was performed in order to quantify the difference between the simulated and experimental profiles at each time interval. Figure 2 depicts LTE (left column), stead-state NLTE (central column), and time-dependent collisional–radiative (CR) modeling (right column). By averaging the R^2 analysis over all times, it was found that the non-LTE models gave the best match to the data. The full CR model appears to capture the early-time dynamics better—the shock amplitude and width closely resemble the experiment—although it slightly over predicts the amplitude of the peak on-axis, while at later times the steady-state NLTE model is better.

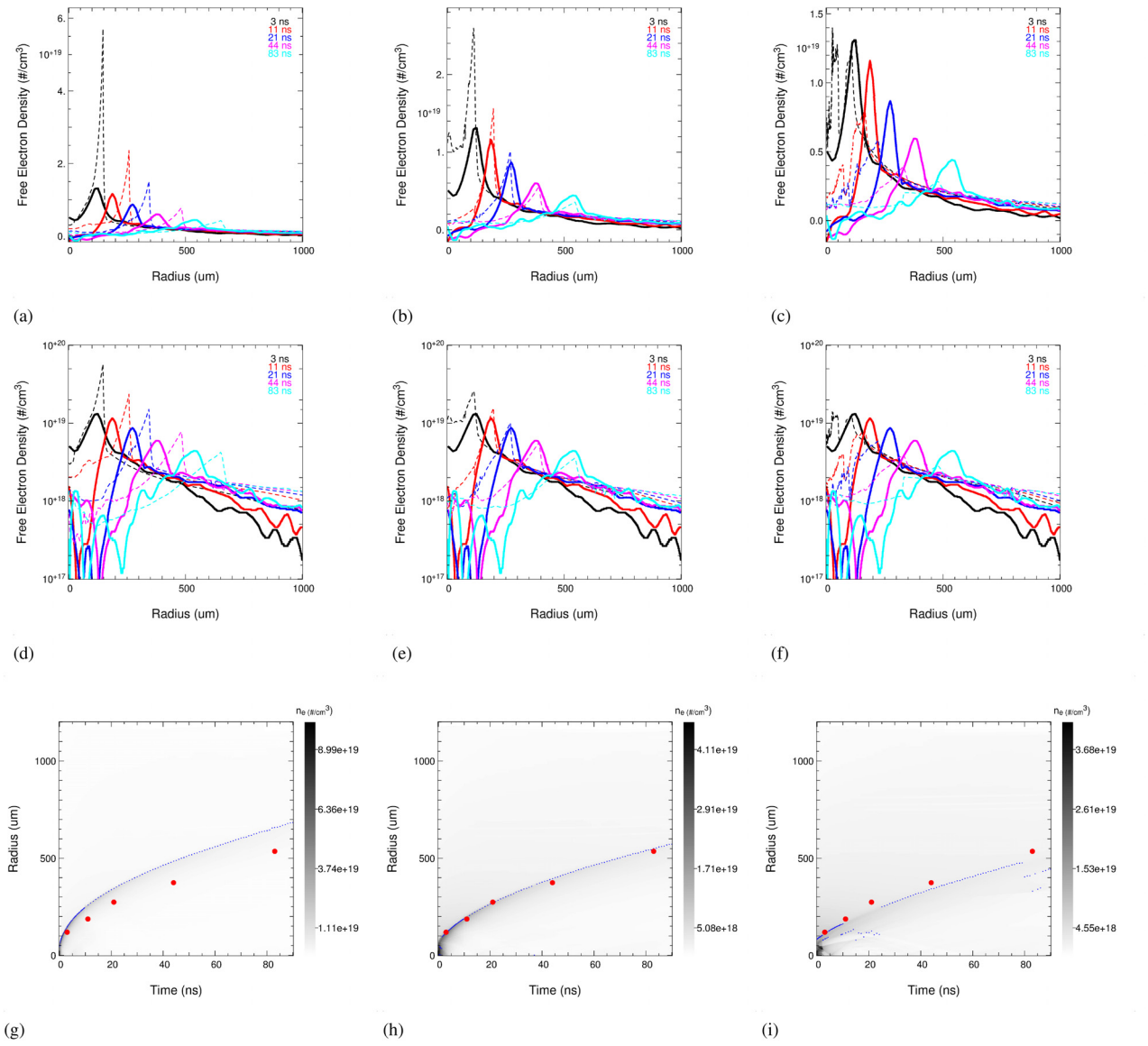

FIG. 2. Top row [(a)–(c)] shows Hyades simulation data (dashed lines) over plotted on the experimental data (solid lines). Middle row [(d)–(f)] is the same data but plotted on a logarithmic scale in order to highlight the precursor region. Bottom row [(g)–(i)] shows the simulated shock trajectory (blue points) over plotted on the experimental shock trajectory (red points). Simulations in the left column [(a), (d), and (g)] use LTE opacities, the central column [(b), (e), and (h)] use a steady state non-LTE atomic model to generate the opacities, while the right column [(c), (f), and (i)] uses a time dependent non-LTE atomic model to generate the opacity data. The steady state non-LTE simulation (central column) was tuned to best match the data by changing the internal energy initially deposited in the electrons. The LTE and time dependent non-LTE runs used exactly the same initial conditions as the steady state non-LTE simulation. It can be seen that in going from LTE, to steady state non-LTE, and finally to time dependent non-LTE, the simulated shocks are systematically reduced in amplitude, increased in width, and propagated more slowly. Note that the gap in the tracked shock trajectory in (i) is due to the shock tracking algorithm being unable to distinguish between the two peaks, as shown by the black dotted line in (c).

In a detailed analysis of the data from the same experiment, Rodriguez *et al.*[2] indicate that the switch to NLTE conditions occurs above 12 eV for the density in these simulations. One interpretation of the CR simulations, which use the 12 eV LTE to NLTE transition temperature, is that the NLTE model over predicts the plasma emissivity at late times (the simulated plasma temperature is above 12 eV until ~30 ns) and hence underestimates the shock amplitude. By increasing the LTE to NLTE transition temperature to 35 eV, it was possible to obtain a better match to the late time data, as shown in Fig. 3. It should be noted that the necessity to use an elevated LTE to NLTE transition temperature does not mean that the transition temperature quoted by Rodriguez *et al.* is incorrect, merely that this value gives a better match to data in the necessarily simplified atomic models employed in radiation-hydrodynamic modeling. Nonetheless, an elevated transition temperature is also consistent with the requirement within the simulations to have a higher initial background density—the McWhirter criterion shows that higher density plasmas have higher LTE to NLTE transition temperatures. However, the peak amplitude at 3 ns was slightly higher than that obtained experimentally. A part of this observed discrepancy in the peak amplitude may be explained by the experimental spatial resolution, which was approximately 125 μm/pixel, resulting in some spatial smoothing of smaller scale and potentially higher density features. This would also bring the early-time steady-state NLTE toward the experimental data.

III. DISCUSSION

In Sec. II, it was found that the best match to the experimental data was obtained with a LTE to NLTE transition temperature of 35 eV. Furthermore, if LTE conditions are assumed to exist, when in fact they do not, the shock velocity is shown to be significantly over predicted by all of the codes used in this study.[21,22]

The best match obtained with the steady-state NLTE model is shown in the central column of Figs. 2(b), 2(e), and 2(h). Using identical initial conditions, this run was repeated with LTE opacities [Figs. 2(a), 2(d), and 2(g)] and the full CR model [Figs. 2(c), 2(f), and 2(i)] in order to evaluate the effects of the various opacity models. Comparing the three runs reveals a trend; in going from LTE, to steady state non-LTE, and finally to time dependent non-LTE, the simulated shocks are systematically reduced in amplitude, increased in width, and reduced in propagation velocity, while the amplitude of the radiative precursor is increased. This trend is consistent with the radiating plasma within the shock being increasingly emissive with the more sophisticated and accurate non-LTE atomic models. As the more emissive models will couple to the precursor, this may explain the requirement to have an elevated simulated density.

As discussed above, the best match to the experimental data was obtained with a time dependent NLTE model. However, it was also shown that the ability to reproduce the experimental data was dependent on the assumed LTE to NLTE transition temperature. This necessity to prescribe an LTE to NLTE transition temperature in radiation-hydrodynamics codes (this is a common feature, not restricted to Hyades) is a significant limitation in current simulation codes' predictive capabilities. The addition of physics models to better describe this transition in radiation-hydrodynamics simulations would be a welcome development.

The experimental shock trajectory was reproducible with relative ease in comparison to the more restrictive electron density profiles. This was possible with the LTE, steady state non-LTE, and time dependent non-LTE models, although the initial conditions required to create the shock trajectory differed significantly, an example of which is detailed in Fig. 4. Furthermore, even with a given simulation opacity/atomic model setup, it was possible to reproduce the shock trajectory with a range of density/internal energy initial conditions, illustrating that the shock trajectory is a degenerate, or non-unique, measure of the initial conditions. This is illustrated in Fig. 4 which shows two simulations, both of which approximately match the experimental shock trajectory [Figs. 4(a) and 4(b)], while the electron density profiles in Fig. 4(c) are quite different.

The radiation-hydrodynamic simulations used to model this experiment ignore the detailed kinetics of the laser–cluster interaction, which govern the initial short-time scale energy deposition into the system, but not those of the atomic physics, assuming instead a heated filament with a Gaussian profile. Although these initial conditions are clearly an approximation, it was found that the radiation-hydrodynamics were relatively insensitive to changes in the assumed initial conditions, leading to

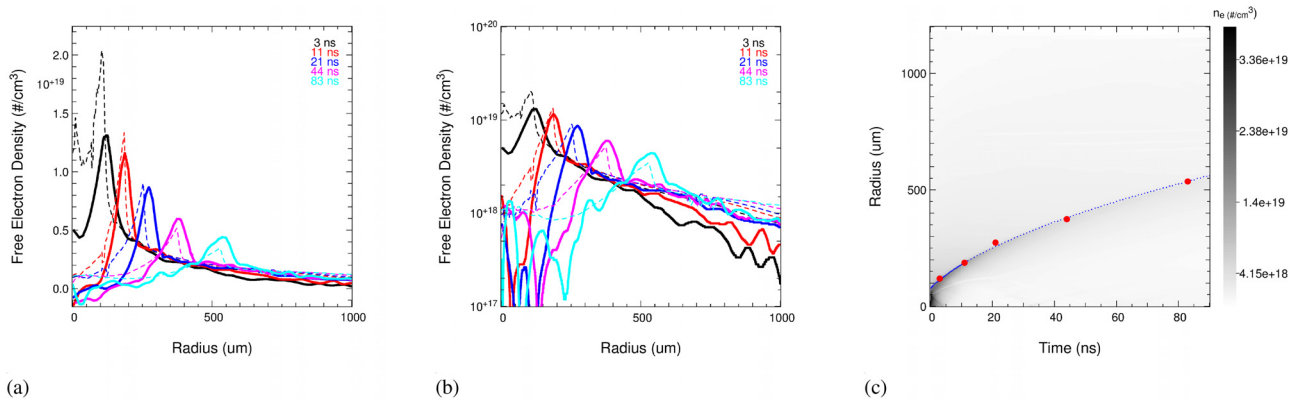

FIG. 3. (a) Hyades simulation data (dashed lines) over plotted on the experimental data (solid lines). (b) As per (a), but with logarithmic y scale to highlight the discrepancy in the precursor region. (c) shows the simulated shock trajectory (blue points) over plotted on the experimental shock trajectory (red points). This simulation was performed using the time dependent non-LTE model with an LTE transition temperature of 35 eV. Despite the peak simulated electron density at 3 ns exceeding the experimental data, this was the best fit obtained.

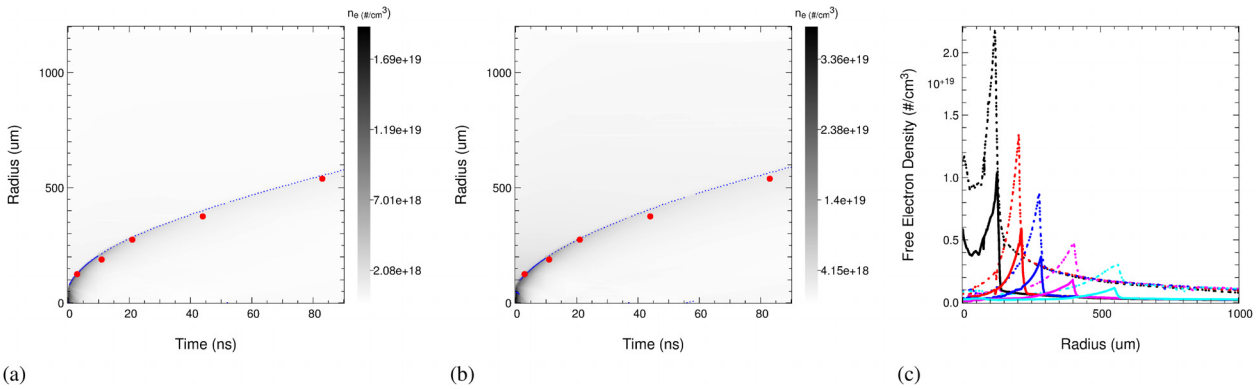

FIG. 4. (a) and (b) show steady state non-LTE Hyades simulations overlaid on the experimental shock trajectory (red points). Both simulations have almost identical shock trajectories, but the initial conditions, which generated these trajectories, were quite different: (a) has an internal energy of 0.3 J and a density of 4.1×10^{-4} g cm^{-3}, while (b) has an internal energy of 0.1 J and a density of 1.6×10^{-4} g cm^{-3}. (c) shows the associated electron density profiles at various times; the dotted lines are from the simulation shown in (a), while the solid lines correspond to the simulation shown in (b). This finding shows that shock trajectory alone is a degenerate measure of the initial conditions.

the tentative conclusion that after the initial laser–cluster interaction (non-atomic/radiative), kinetics play a relatively unimportant role in the subsequent shock formation and propagation.

The initial gas consists of atomic clusters, not a uniform gas, as assumed in the radiation-hydrodynamics simulations. Interestingly, the diffusive radiation transport approximation employed throughout this work would be expected to be better in a cluster–gas than an equivalent average density gas, due to the repeated absorption and re-emission caused by the locally over-dense clusters. At early-times, clusters will exist; however, by 3 ns (the time of the first experimental electron density lineout), the data suggests that they have been destroyed;[24,25] even on the edge of the experimental field of view, a plasma exists with $Z^* \sim 1$. Previous work[25] suggests that the clusters are broken up by the fast ions from the initial interaction before the shock arrives. The leads us to the tentative conclusion that using a homogeneous gas as the initial conditions for the hydrodynamics is the most probably adequate.

The finding that non-LTE physics is of importance to the accurate description of these radiative-shocks has implications for laboratory astrophysics experiments which enter the radiative-shock regime. The scalings, which are used to transform from the laboratory to the astrophysical scale, do not, as far as the authors are aware, hold for non-LTE systems. Therefore, laboratory–astrophysics experiments which seek to explore radiative-shocks should be aware of the limitations that this places on the validity of the extrapolation of such experiments to astrophysical scales. This is highlighted in this work which finds the conditions to be non-LTE, despite relatively modest temperatures and elevated densities in comparison with astrophysical regimes.

IV. CONCLUSIONS

Radiative-shocks induced by laser–cluster interactions are an extremely challenging experimental scenario to model numerically due to their disparate spatio-temporal scales, complex early time kinetics, high electron temperatures, and low density. The radiation-hydrodynamic modeling performed here indicates that non-LTE atomic-kinetics are an important factor in the accurate description of the energy balance of the radiative-shocks examined experimentally. This is particularly true at early times due to the elevated temperatures.

A range of issues associated with the successful modeling of such scenarios have been identified and discussed, including the effects of the various atomic models used to generate the opacity data (LTE/steady state non-LTE/collisional–radiative non-LTE). In going from LTE, to steady state non-LTE, and finally to time dependent non-LTE, the simulated shocks are systematically reduced in amplitude, increased in width, and reduced in propagation velocity, while the amplitude of the radiative precursor is increased. This trend is broadly consistent with the radiative-shock being increasingly emissive with the more sophisticated and accurate non-LTE atomic models. Furthermore, it has been shown that the induced shock trajectory is degenerate in relation to the plasma initial conditions.

Laboratory–astrophysics experiments, which seek to explore radiative-shocks in this regime, should be aware of the limitations that the requirement of LTE places on the validity of their experiments, as the scalings employed to transform from laboratory to astrophysical scales do not hold for non-LTE systems.

ACKNOWLEDGMENTS

The authors would like to thank J. Fyrth for his valuable contributions to this work. We gratefully acknowledge supporting funding from EPSRC Grant No. EP/G001324/1, EPSRC doctoral training account, and AWE Aldermaston Industrial CASE Studentships.

REFERENCES

[1]S. Bouquet, E. Falize, C. Michaut, C. Gregory, B. Loupias, T. Vinci, and M. Koenig, "From lasers to the universe: Scaling laws in laboratory astrophysics," High Energy Density Phys. **6**(4), 368–380 (2010).
[2]R. Rodriguez, G. Espinosa, J. Gil, R. Florido, J. Rubiano, M. Mendoza, P. Martel, E. Minguez, D. Symes, M. Hohenberger, and R. Smith, "Analysis of microscopic magnitudes of radiative blast waves launched in xenon clusters with collisional-radiative steady-state simulations," J. Quant. Spectrosc. Radiat. Transfer **125**(0), 69–83 (2013).
[3]A. R. Bell, "The acceleration of cosmic rays in shock fronts—I," Mon. Not. R. Astron. Soc. **182**(2), 147–156 (1978).
[4]A. R. Bell, "Turbulent amplification of magnetic field and diffusive shock acceleration of cosmic rays," Mon. Not. R. Astron. Soc. **353**(2), 550–558 (2004).

[5]J. Grun, J. Stamper, C. Manka, J. Resnick, R. Burris, J. Crawford, and B. H. Ripin, "Instability of Taylor-Sedov blast waves propagating through a uniform gas," Phys. Rev. Lett. **66**, 2738–2741 (1991).
[6]S. Bouquet, C. Stéhlé, M. Koenig, J.-P. Chièze, A. Benuzzi-Mounaix, D. Batani, S. Leygnac, X. Fleury, H. Merdji, C. Michaut, F. Thais, N. Grandjouan, T. Hall, E. Henry, V. Malka, and J.-P. J. Lafon, "Observation of laser driven supercritical radiative shock precursors," Phys. Rev. Lett. **92**, 225001 (2004).
[7]J. F. Hansen, M. J. Edwards, D. H. Froula, G. Gregori, A. D. Edens, and T. Ditmire, "Laboratory observation of secondary shock formation ahead of a strongly radiative blast wave," Phys. Plasmas **13**(2), 022105 (2006).
[8]A. D. Edens, R. G. Adams, P. Rambo, L. Ruggles, I. C. Smith, J. L. Porter, and T. Ditmire, "Study of high Mach number laser driven blast waves in gases," Phys. Plasmas **17**(11), 112104 (2010).
[9]M. J. Edwards, A. J. MacKinnon, J. Zweiback, K. Shigemori, D. Ryutov, A. M. Rubenchik, K. A. Keilty, E. Liang, B. A. Remington, and T. Ditmire, "Investigation of ultrafast laser-driven radiative blast waves," Phys. Rev. Lett. **87**, 085004 (2001).
[10]K. Shigemori, T. Ditmire, B. A. Remington, V. Yanovsky, D. Ryutov, K. G. Estabrook, M. J. Edwards, A. J. MacKinnon, A. M. Rubenchik, K. A. Keilty, and E. Liang, "Developing a radiative shock experiment relevant to astrophysics," Astrophys. J. Lett. **533**(2), L159 (2000).
[11]A. Pak, L. Divol, G. Gregori, S. Weber, J. Atherton, R. Bennedetti, D. K. Bradley, D. Callahan, D. T. Casey, E. Dewald, T. Doppner, M. J. Edwards, J. A. Frenje, S. Glenn, G. P. Grim, D. Hicks, W. W. Hsing, N. Izumi, O. S. Jones, M. G. Johnson, S. F. Khan, J. D. Kilkenny, J. L. Kline, G. A. Kyrala, J. Lindl, O. L. Landen, S. L. Pape, T. Ma, A. MacPhee, B. J. MacGowan, A. J. MacKinnon, L. Masse, N. B. Meezan, J. D. Moody, R. E. Olson, J. E. Ralph, H. F. Robey, H.-S. Park, B. A. Remington, J. S. Ross, R. Tommasini, R. P. J. Town, V. Smalyuk, S. H. Glenzer, and E. I. Moses, "Radiative shocks produced from spherical cryogenic implosions at the National Ignition Facility," Phys. Plasmas **20**(5), 056315 (2013).
[12]R. A. Smith, T. Ditmire, and J. W. G. Tisch, "Characterization of a cryogenically cooled high-pressure gas jet for laser/cluster interaction experiments," Rev. Sci. Instrum. **69**(11), 3798–3804 (1998).
[13]T. Ditmire, E. Springate, J. W. G. Tisch, Y. L. Shao, M. B. Mason, N. Hay, J. P. Marangos, and M. H. R. Hutchinson, "Explosion of atomic clusters heated by high-intensity femtosecond laser pulses," Phys. Rev. A **57**, 369–382 (1998).
[14]T. Ditmire, R. A. Smith, J. W. G. Tisch, and M. H. R. Hutchinson, "High intensity laser absorption by gases of atomic clusters," Phys. Rev. Lett. **78**, 3121–3124 (1997).
[15]M. Hohenberger, D. R. Symes, J. Lazarus, H. W. Doyle, R. E. Carley, A. S. Moore, E. T. Gumbrell, M. M. Notley, R. J. Clarke, M. Dunne, and R. A. Smith, "Observation of a velocity domain cooling instability in a radiative shock," Phys. Rev. Lett. **105**, 205003 (2010).
[16]J. Osterhoff, D. R. Symes, A. D. Edens, A. S. Moore, E. Hellewell, and T. Ditmire, "Radiative shell thinning in intense laser-driven blast waves," New J. Phys. **11**(2), 023022 (2009).
[17]R. Zel'Dovich, *Physics of Shock Waves and High-Temperature Hydrodynamic Phenomena* (Dover, 2001).
[18]G. Cristoforetti, A. D. Giacomo, M. Dell'Aglio, S. Legnaioli, E. Tognoni, V. Palleschi, and N. Omenetto, "Local thermodynamic equilibrium in laser-induced breakdown spectroscopy: Beyond the mcwhirter criterion," Spectrochim. Acta B: At. Spectrosc. **65**(1), 86–95 (2010).
[19]R. McWhirter and R. Huddlestone, *Plasma Diagnostic Techniques* (Academic Press, 1965).
[20]D. R. Bates, A. E. Kingston, and R. W. P. McWhirter, "Recombination between electrons and atomic ions. I. Optically thin plasmas," Proc. R. Soc. London., A: Math. Phys. Sci. **267**(1330), 297–312 (1962).
[21]M. M. Marinak, G. D. Kerbel, N. A. Gentile, O. Jones, D. Munro, S. Pollaine, T. R. Dittrich, and S. W. Haan, "Three-dimensional hydra simulations of national ignition facility targets," Phys. Plasmas **8**(5), 2275–2280 (2001).
[22]J. J. MacFarlane, I. E. Golovkin, and P. R. Woodruff, "HELIOS-CR—A 1-D radiation-magnetohydrodynamics code with inline atomic kinetics modeling," J. Quant. Spectrosc. Radiat. Transfer **99**(1–3), 381–397 (2006).
[23]J. T. Larsen and S. M. Lane, "Hyades—A plasma hydrodynamics code for dense plasma studies," J. Quant. Spectrosc. Radiat. Transfer **51**(1–2), 179–186 (1994).
[24]A. S. Moore, E. T. Gumbrell, J. Lazarus, M. Hohenberger, J. S. Robinson, R. A. Smith, T. J. A. Plant, D. R. Symes, and M. Dunne, "Full-trajectory diagnosis of laser-driven radiative blast waves in search of thermal plasma instabilities," Phys. Rev. Lett. **100**, 055001 (2008).
[25]S. O. Robbie, H. Doyle, D. Symes, and R. Smith, "A study of ambient upstream material properties using perpendicular laser driven radiative blast waves in atomic cluster gases," High Energy Density Phys. **8**(1), 55–59 (2012).